第 43 卷 第 5 期/2023 年 3 月/光学学报 研究论文

光学学报

2.15 μm全光纤气体拉曼激光光源

李子颜[1]，裴闻喜[1,2]，李昊[1,2]，黄威[1,2]，李炫熹[1,2]，王泽锋[1,2,3*]，陈金宝[1,2,3]

[1]国防科技大学前沿交叉学科学院，湖南 长沙 410073；

[2]国防科技大学南湖之光实验室，湖南 长沙 410073；

[3]脉冲功率激光技术国家重点实验室，湖南 长沙 410073

摘要 报道了全光纤2.15 μm波段光纤气体拉曼激光器。将实芯单模光纤与空芯光子晶体光纤直接熔接制备成全光纤气体腔，并在实芯光纤上刻写长周期光纤光栅，防止菲涅耳反射回光对泵浦源造成损坏。以1971 nm脉冲光纤放大器作为泵浦源，当腔内气压为1.4 GPa时，2.15 μm拉曼光的最大平均功率约为0.87 W，受限于较高的拉曼阈值，光光转换效率只有19%。本研究为实现2.15 μm光纤激光光源提供了一种新的可行的技术方案。

关键词 激光器；光纤气体拉曼激光器；空芯光纤；受激拉曼散射

中图分类号 TN248 **文献标志码** A **DOI**：10.3788/AOS221692

1 引 言

2 μm波段激光光源在众多领域中有着广泛的应用：该波段激光位于大气传输窗口，并且对烟雾透射能力强，在某些特殊情境下作为通信波段更为可靠[1]；已有文献报道该波段的激光雷达可实现对大气环境的测量[2]；2 μm波段激光光源也是ZGP、GaAs和$BaGa_4Se_7$等晶体通过非线性变频产生中红外激光的理想泵浦源[3-5]；在加工有机聚合物材料领域中[6]，2 μm波段激光也有特殊的优势。

目前主要通过掺铥光纤激光器（TDFL）和掺钬光纤激光器（HDFL）产生2 μm波段光纤激光，利用Tm^{3+}和Ho^{3+}的能级跃迁实现激光输出。由于Tm^{3+}和Ho^{3+}在2.1 μm以上波段内的吸收截面和发射截面急剧减小[7]，故波长难以拓展至更长波长。2009年，首个2106 nm掺钬光纤脉冲激光器被报道，利用增益开关掺铥光纤激光器泵浦掺钬光纤，实现了平均功率仅为0.25 W的脉冲输出[8]。2012年，Hollitt等[9]利用放大后的1550 nm脉冲级联泵浦掺钬光纤，在2104 nm处实现了5.1 W的功率输出。2018年，Yao等[10]基于主振荡功率放大器（MOPA）结构在2116 nm处实现了99 W的平均功率输出。虽然在功率上有所突破，但是对于传统的利用能级跃迁产生2 μm光纤激光的HDFL和TDFL，高泵浦功率下的自相位调制和受激拉曼散射等非线性效应会引起光谱展宽[11]，同时复杂的系统对热处理提出了较高的要求，一定程度上限制了其应用。

光纤气体拉曼激光器是基于空芯光纤中气体受激拉曼散射的新型光纤激光器[12]，是拓展光纤激光器输出波长，实现窄线宽激光输出[13]的一种新的有效的技术方案。自2002年首次被报道以来[14]，已经有不同波段的光纤气体拉曼激光器被报道[15-26]。2004年，Benabid等[15]报道了基于氢气受激拉曼散射的1135 nm光纤气体拉曼激光器，量子效率达到了92%。2014年，本课题组与巴斯大学合作，利用1064 nm激光作为泵浦源，泵浦充入反谐振空芯光纤中的氢气，实现了光纤气体拉曼激光器1.9 μm波段激光输出[16]，峰值功率超过2 kW，转换效率为27%。2016年，本课题组报道了基于乙烷的1.5 μm光纤气体拉曼激光器[17]，峰值功率超过400 kW。2017年，Gladyshev等[18]利用氢气的振动受激拉曼散射实现了4.4 μm光纤气体拉曼激光器，随后通过优化泵浦源的方式将功率提升至瓦级[20]。2020年，本课题组报道了1.7 μm光纤气体拉曼激光器[21]。同年，Wang等[22]利用二氧化碳实现了1.95 μm的高脉冲能量输出。然而，以往的报道大多数是通过空间耦合的方式将泵浦光耦合进空芯光纤中，本课题组于2021年报道了连续波1.7 μm全光纤气体拉曼激光器[27]，目前鲜有关于2.15 μm波段光纤气体激光器的报道。本文利用实芯光纤与空芯光纤熔接，使得激光器系统更加稳定紧凑，并在光纤气体拉曼

收稿日期：2022-09-09；**修回日期**：2022-10-10；**录用日期**：2022-10-17；**网络首发日期**：2022-10-27

基金项目：国家自然科学基金（11974427，12004431）、脉冲功率激光技术国家重点实验室主任基金（SKL2020ZR05，SKL2021ZR01）、湖南省研究生科研创新项目（CX20200004）

通信作者：*zefengwang_nudt@163.com

激光器中引入自行刻写的长周期光纤光栅有效防止了熔点的菲涅耳反射对泵浦源造成损伤。

报道了全光纤结构的2.15 μm光纤气体拉曼激光光源。使用电弧放电熔接机将实芯单模光纤与空芯光子晶体光纤(HC-PCF)熔接,引入紫外刻写的长周期光纤光栅制备了全光纤气体腔,可有效防止熔点的菲涅耳反射对泵浦源造成损伤。利用1971 nm脉冲放大器作为泵浦源,当长度为25.8 m的全光纤气体腔内的气压为1.4 GPa时,调节泵浦光的重复频率和脉冲宽度可获得的最大拉曼功率约为0.87 W,光光转换效率为19%。本研究为实现窄线宽的2.15 μm光纤激光光源提供了一种新的技术方案。

2　实验装置

2.1　实验系统

图1(a)为2.15 μm全光纤气体拉曼激光器实验系统示意图。泵浦源是一个1971 nm脉冲光纤放大器,由种子源(Advanced Photonics,AP-TM-165)、调制器(NPI Lasers,Rainbow-2000-NS)和放大器(NPI Lasers,TDFA-HP)组成,种子源光谱如图1(b)所示。泵浦光能通过调制器调制成不同重复频率(0.5~2.2 MHz)和脉冲宽度(10~30 ns)的脉冲光,调制后的脉冲经放大器放大后输出。放大器的输出尾纤(SMF-28e)与一个光纤分束器(SMF-28e)相连用来实时监测泵浦功率。光纤分束器的主输出纤与一根实芯单模光纤(NUFERN,SMF-10/125)熔接,再将其与空芯光纤相熔接。将SMF-10/125光纤作为过渡光纤的目的在于减小因模场不匹配而导致的熔接损耗(Splice 2处),经测量,实芯光纤到空芯光纤的熔接损耗约为1.42 dB。输入端长周期光栅(LPG)的功能是在2.15 μm处引入较高的损耗,防止熔点菲涅耳反射的拉曼光对泵浦源造成损伤,透射光谱如图1(c)所示。长周期光栅的周期为0.6 mm,周期数为60,经测试其在泵浦光波段的插入损耗约为0.6 dB。从图1(c)可以看出,长周期光栅在2147 nm处的凹陷深度约为−8 dBm,即菲涅耳反射产生的绝大部分(约85%)拉曼回光经过长周期光栅后会被损耗,能够很好地防止泵浦源因拉曼回光而产生损坏。激光通过玻璃窗口(Thorlabs,WG-61050)输出后,经透镜(Thorlabs,LA-1560D)准直,利用可翻转的镀银反射镜可实现光谱的测量,通过翻转架上的滤波片(Thorlabs,FB2250-500)可实现对拉曼功率和总功率的测量。

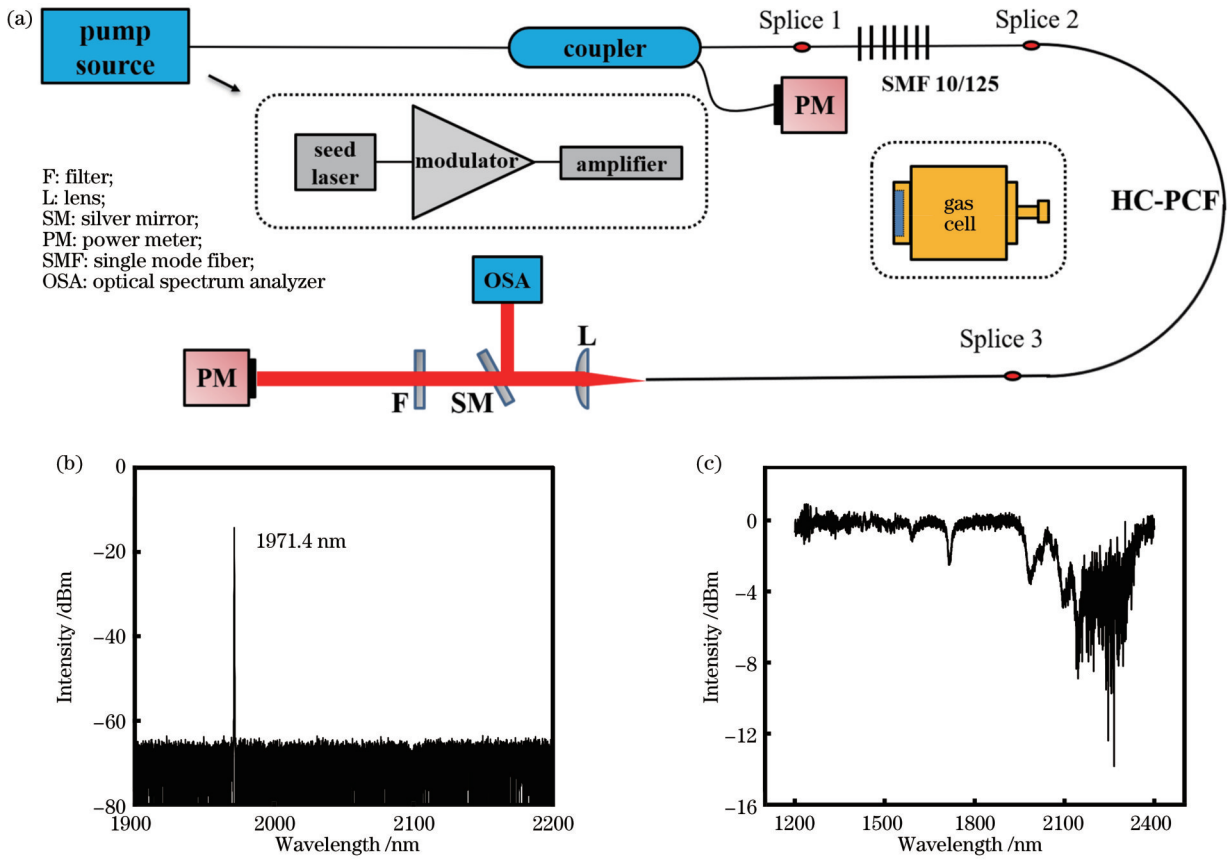

图1　2.15 μm全光纤气体拉曼激光器示意图。(a)系统结构;(b)种子源光谱;(c)长周期光栅透射光谱

Fig. 1　Experimental setup of 2.15 μm all-fiber gas Raman laser. (a) Configuration of system; (b) spectrum of seed laser; (c) transmittance spectrum of long-period fiber grating

2.2　空芯光子晶体光纤和全光纤气体腔

图2(a)是利用超连续谱源通过截断法测量得到的空芯光纤(NKT Photonics,HC-2000-01)传输损耗谱。可以看到,空芯光纤在1950~2160 nm波长范围内有较

低的传输损耗，且该空芯光纤在1971 nm和2147 nm处的损耗分别为0.075 dB/m和0.21 dB/m。图2(b)是空芯光纤横截面的光学显微镜图：纤芯直径约为15 μm，对应模场直径约为10 μm，与SMF-10/125的模场直径相近；空芯光纤包层直径约为155 μm，数值孔径约为0.2，盘绕半径约为11 cm。图2(c)是实芯光纤与空芯光纤熔接的光学显微镜图。由于空芯光纤特殊的微空气孔结构，故在利用电弧放电熔接机(Fujikura，80S)进行熔接时，需要调整熔接机的放电强度、放电时间和放电位置，尽可能减小对空芯光纤微结构的损坏，以达到减小熔接损耗的目的。经过不断调整参数，实芯光纤到空芯光纤的熔接损耗可降低至1.42 dB。

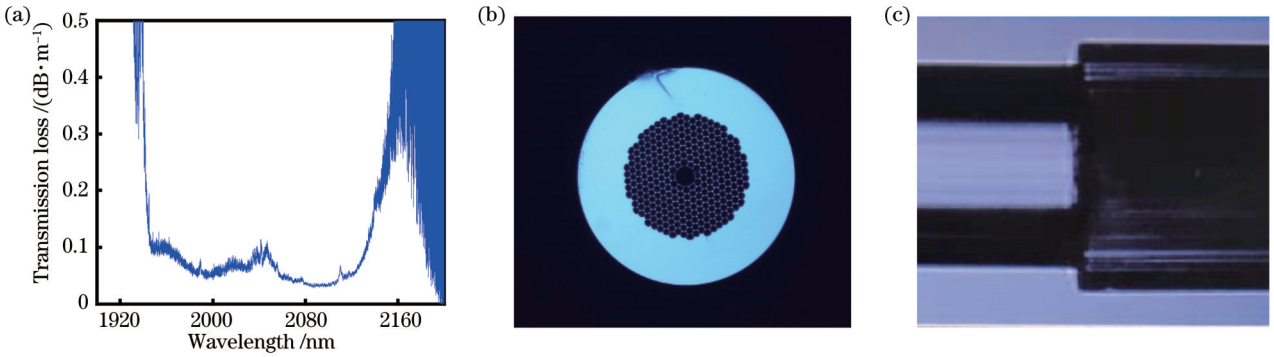

图2 实验结果。(a)测量所得空芯光纤传输损耗谱；(b)空芯光纤横截面显微镜图；(c)Splice 2处放大图

Fig. 2 Experimental results. (a) Measured transmission loss spectrum of hollow core fiber; (b) microscopic view of cross-section of hollow-core fiber; (c) enlarged view of Splice 2

将空芯光纤输出端密封在图1(a)所示的气体腔中，再通过气体腔对空芯光纤进行抽真空和充气操作，向空芯光纤中充入一定气压的氘气，待平衡后将空芯光纤取出，迅速将其与实芯光纤熔接，从而完成全光纤气体腔的制备，从空芯光纤到实芯光纤的熔接损耗约为1 dB(Splice 3处)。熔接过程中会有漏气，最终气体腔中的气压可以由计算获得[28]，通过计算得知全光纤气体腔中氘气气压约为1.4 GPa。

3 实验结果与分析

3.1 光谱特性

泵浦光波长与拉曼光波长之间的关系可以表示为

$$\Delta\left(\frac{1}{\lambda}\right)=\frac{1}{\lambda_p}-\frac{1}{\lambda_s}, \tag{1}$$

式中：λ_p为泵浦波长；λ_s为拉曼光波长；$\Delta(1/\lambda)$为拉曼频移。当已知泵浦光波长时，通过将拉曼频移数值代入，即可得到相应的拉曼光波长。图3(a)为泵浦脉冲宽度为10 ns、重复频率为1.5 MHz时输出光谱随注入泵浦功率(Splice 1之前)的变化，图3(b)～(d)是三条谱线的精细谱，其中心波长分别为1971.5 nm(泵浦光)、2043.6 nm(一阶拉曼，对应的拉曼频移为179 cm^{-1})和2147.1 nm(一阶拉曼，对应的拉曼频移为414 cm^{-1})。从图3(a)可以看出，随着泵浦功率的升高，波长为2147.1 nm的一阶拉曼最先出现，光谱中含有的2043.6 nm拉曼光成分较微弱，且其强度比2147.1 nm拉曼光的强度小20 dB以上。因此，本文所指拉曼功率均为2147.1 nm拉曼光的功率。

图4(a)、(b)分别是不同重复频率(脉冲宽度为10 ns)拉曼光功率和残余泵浦光功率随耦合泵浦功率的变化。由于受到放大器本身安全的限制，故其在不同重复频率下的最大输出功率不同。因此，图4中不同重复频率下最大耦合泵浦功率也不同。可以看出，随着重复频率的增加，拉曼阈值也在逐渐增大，原因是重复频率的增加导致泵浦光峰值功率下降，需要平均功率更高的泵浦光才能达到产生拉曼光的阈值。图4(c)为光光转换效率(拉曼光功率与耦合泵浦功率的比值)随耦合泵浦功率的变化情况。当重复频率为1.5 MHz、脉冲宽度为10 ns时，2147.1 nm处的最大拉曼功率为0.84 W，对应光光转换效率约为19%。在本实验中光光转换效率较低，原因在于氘气转动频移(414 cm^{-1})的拉曼增益较低[29]和低气压造成的较大拉曼阈值。后续可以通过优化空芯光纤长度、继续优化熔接损耗和进一步提高腔内气压来提高转换效率进而提高系统的输出功率。

图5(a)、(b)是当泵浦光重复频率为1.5 MHz时不同脉冲宽度的拉曼光功率和残余泵浦光功率曲线。可以看出，随着脉冲宽度的增加，拉曼阈值逐渐增大，最大拉曼功率也随之下降，原因在于脉冲宽度的增加会导致泵浦光脉冲的峰值功率降低，而泵浦脉冲中只有峰值功率超过拉曼阈值的部分才能转化为拉曼光。

图6是泵浦光重复频率为1.5 MHz、脉冲宽度为10 ns时测量的泵浦光、拉曼光和残余泵浦光的脉冲序列和形状。从图6(b)可以看出，残余泵浦光脉冲有一个明显的凹陷，这是由该部分泵浦光被转换成拉曼光造成的。拉曼光的脉冲宽度略小于泵浦光，可见所提全光纤气体拉曼激光器也能在一定程度上起到压窄脉宽的作用。

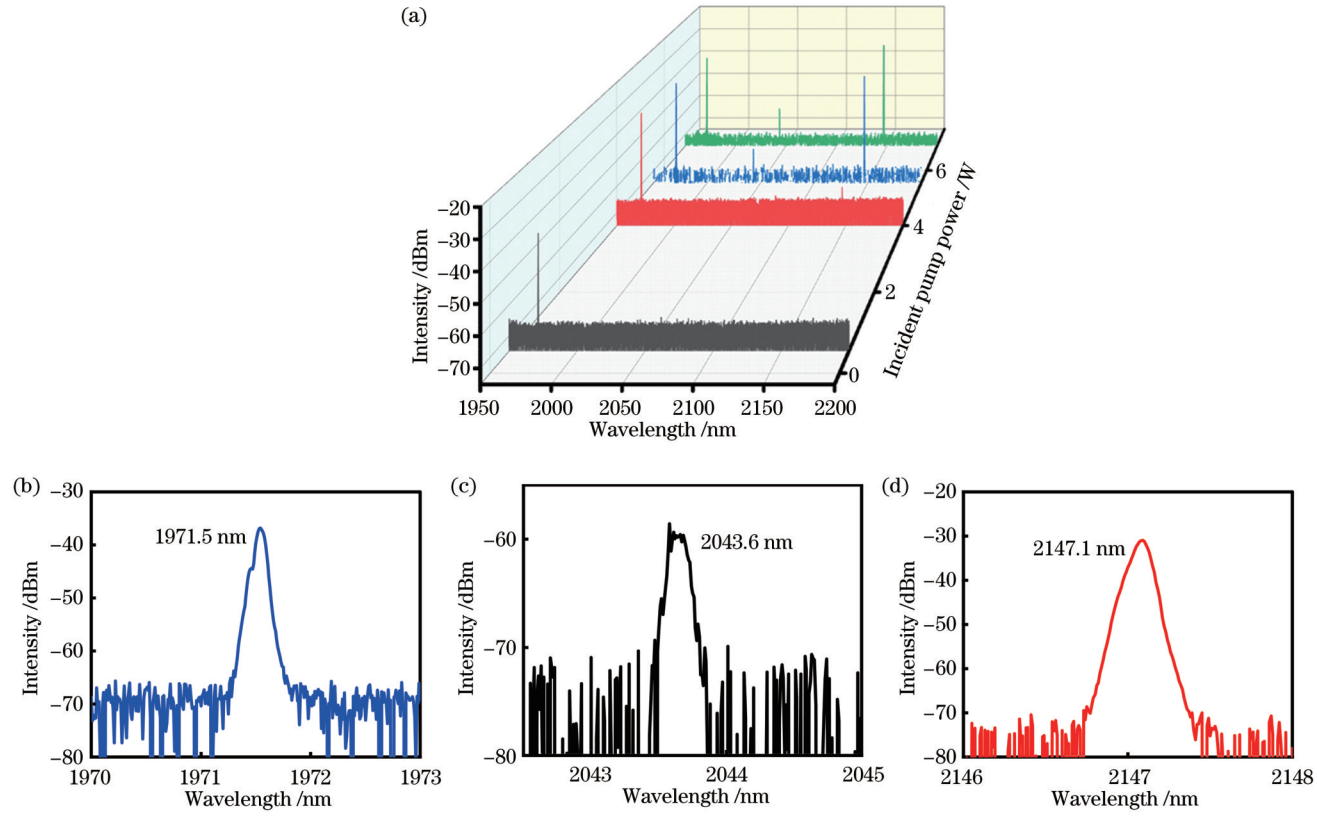

图 3 光谱结果。(a)光谱随注入泵浦功率的变化;(b)泵浦光精细光谱;(c)中心波长为 2043.6 nm 的拉曼光的精细光谱;(d)中心波长为 2147.1 nm 的拉曼光精细光谱

Fig. 3 Spectrum results. (a) Spectrum varying with pump power; (b) fine spectrum of pump laser; (c) fine spectrum of Raman laser with central wavelength of 2043.6 nm; (d) fine spectrum of Raman laser with central wavelength of 2147.1 nm

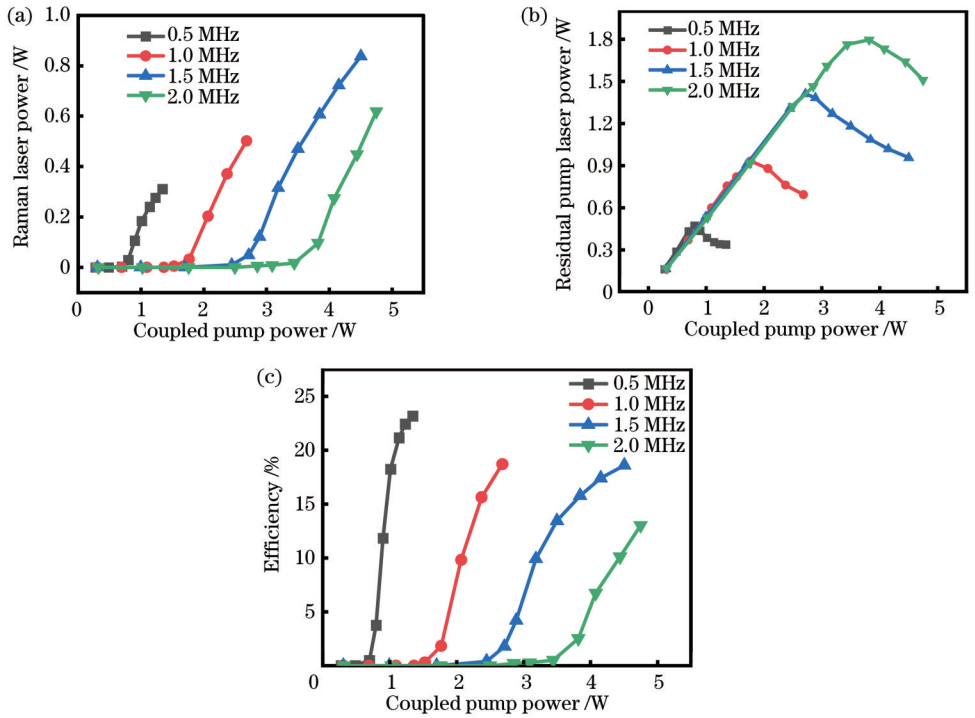

图 4 拉曼光功率、残余泵浦光功率和光光转换效率随耦合泵浦光功率的变化。(a)拉曼光功率;(b)残余泵浦光功率;(c)光光转换效率

Fig. 4 Raman laser power, residual pump laser power and optical-to-optical conversion efficiency varying with coupled pump power. (a) Raman laser power; (b) residual pump laser power; (c) optical-to-optical conversion efficiency

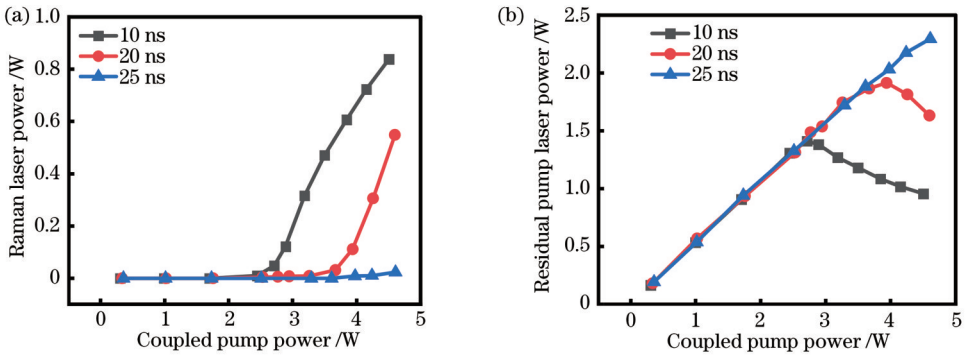

图 5 不同脉宽下功率随耦合泵浦功率的变化。(a)拉曼光;(b)残余泵浦光

Fig. 5 Power varying with coupled pump power under different pulse widths. (a) Raman laser; (b) residual pump laser

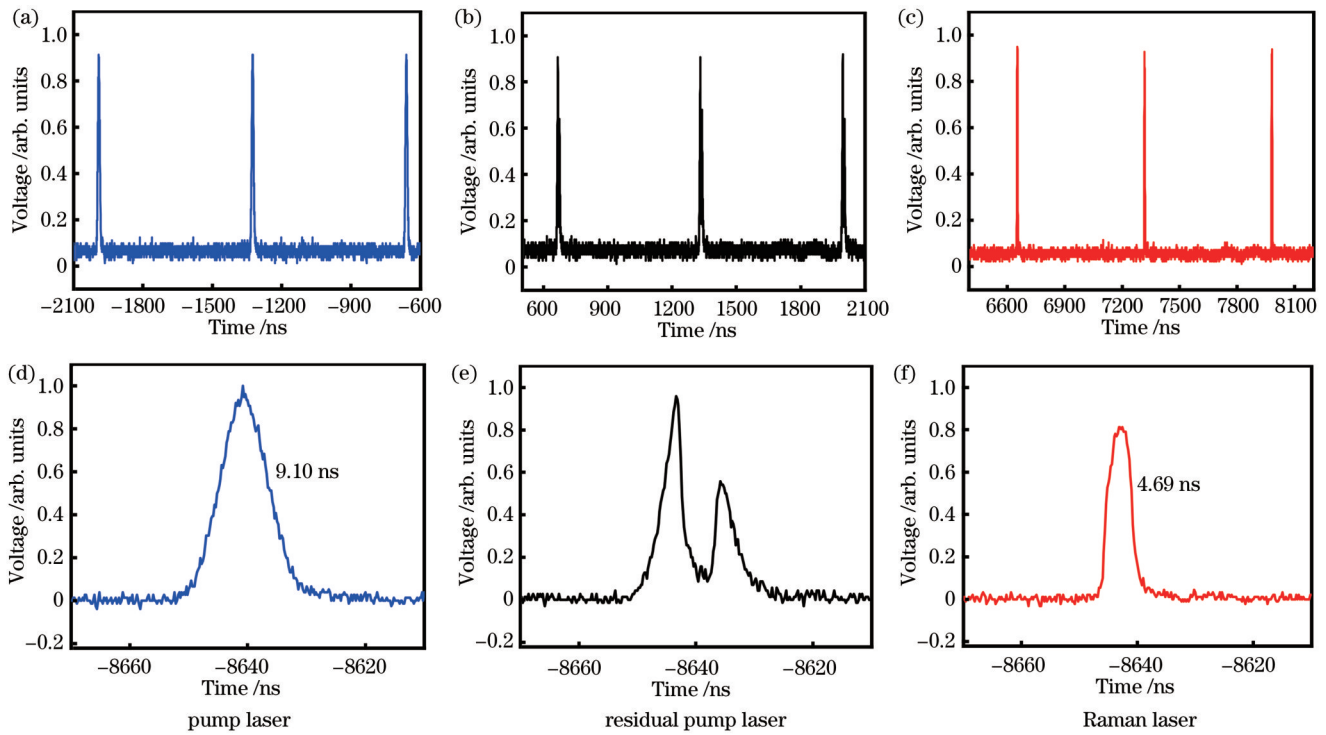

图 6 脉冲序列和脉冲形状。(a)~(c)脉冲序列;(d)~(f)脉冲形状

Fig. 6 Pulse train and pulse profile. (a)-(c) Pulse train; (d)-(f) pulse profile

4 结 论

报道了 2.15 μm 全光纤气体拉曼激光器,引入了自行刻写的 2.15 μm 长周期光纤光栅,制备了全光纤气体腔。当光纤长度为 25.8 m,内部气压为 1.4 GPa 时,最大拉曼功率约为 0.87 W,对应的光光转换效率为 19%。通过优化光纤长度和空芯光纤与实芯光纤间的熔接损耗,可以进一步提高拉曼功率和光光转换效率。未来可分别在输入端和输出端接入泵浦光和拉曼光高反光栅,利用振荡器结构进一步降低拉曼阈值,提高转换效率。本研究为实现 2.15 μm 光纤激光光源提供了一种新的技术方案。

参 考 文 献

[1] Lin P, Wang T S, Ma W Z, et al. Transmission characteristics of 1.55 and 2.04 μm laser carriers in a simulated smoke channel based on an actively mode-locked fiber laser[J]. Optics Express, 2020, 28(26): 39216-39226.

[2] Lahyani J, Le Gouët J, Gibert F, et al. 2.05-μm all-fiber laser source designed for CO_2 and wind coherent lidar measurement [J]. Applied Optics, 2021, 60(15): C12-C19.

[3] Holmen L G, Fonnum H. Holmium-doped fiber amplifier for pumping a $ZnGeP_2$ optical parametric oscillator[J]. Optics Express, 2021, 29(6): 8477-8489.

[4] Yuan J H, Li C, Yao B Q, et al. High power, tunable mid-infrared $BaGa_4Se_7$ optical parametric oscillator pumped by a 2.1 μm Ho∶YAG laser[J]. Optics Express, 2016, 24(6): 6083-6087.

[5] Bloom G, Grisard A, Lallier E, et al. Optical parametric amplification of a distributed feedback quantum cascade laser in orientation-patterned GaAs[J]. Optics Letters, 2010, 35(4): 505-507.

[6] Wood C, Carpenter D, Lyngnes O. Laser damage testing for ion beam sputtered optical coatings at 2 μm and 3 μm[J]. Proceedings of SPIE, 2011, 8039: 803916.

[7] Hemming A, Simakov N, Haub J, et al. A review of recent progress in holmium-doped silica fibre sources[J]. Optical Fiber Technology, 2014, 20(6): 621-630.
[8] Wu K S, Ottaway D, Munch J, et al. Gain-switched holmium-doped fibre laser[J]. Optics Express, 2009, 17(23): 20872-20877.
[9] Hollitt S, Simakov N, Hemming A, et al. A linearly polarised, pulsed Ho-doped fiber laser[J]. Optics Express, 2012, 20(15): 16285-16290.
[10] Yao W C, Shen C F, Shao Z H, et al. High-power nanosecond pulse generation from an integrated Tm-Ho fiber MOPA over 2.1 μm[J]. Optics Express, 2018, 26(7): 8841-8848.
[11] Yan P, Sun J Y, Li D, et al. 933 W Yb-doped fiber ASE amplifier with 50.4 nm bandwidth[J]. Optics Express, 2016, 24(17): 19940-19948.
[12] 王泽锋, 黄威, 李智贤, 等. 光纤气体激光光源研究进展及展望(Ⅰ): 基于受激拉曼散射[J]. 中国激光, 2021, 48(4): 0401008.
Wang Z F, Huang W, Li Z X, et al. Progress and prospects of fiber gas laser sources (Ⅰ): based on stimulated Raman scattering [J]. Chinese Journal of Lasers, 2021, 48(4): 0401008.
[13] Russell P S J, Hölzer P, Chang W, et al. Hollow-core photonic crystal fibres for gas-based nonlinear optics[J]. Nature Photonics, 2014, 8(4): 278-286.
[14] Benabid F, Knight J C, Antonopoulos G, et al. Stimulated Raman scattering in hydrogen-filled hollow-core photonic crystal fiber[J]. Science, 2002, 298(5592): 399-402.
[15] Benabid F, Bouwmans G, Knight J C, et al. Ultrahigh efficiency laser wavelength conversion in a gas-filled hollow core photonic crystal fiber by pure stimulated rotational Raman scattering in molecular hydrogen[J]. Physical Review Letters, 2004, 93(12): 123903.
[16] Wang Z F, Yu F, Wadsworth W J, et al. Efficient 1.9 μm emission in H_2-filled hollow core fiber by pure stimulated vibrational Raman scattering[J]. Laser Physics Letters, 2014, 11(10): 105807.
[17] Chen Y B, Wang Z F, Gu B, et al. Achieving a 1.5 μm fiber gas Raman laser source with about 400 kW of peak power and a 6.3 GHz linewidth[J]. Optics Letters, 2016, 41(21): 5118-5121.
[18] Gladyshev A V, Kosolapov A F, Khudyakov M M, et al. 4.4-μm Raman laser based on hollow-core silica fibre[J]. Quantum Electronics, 2017, 47(5): 491-494.
[19] Cao L, Gao S F, Peng Z G, et al. High peak power 2.8 μm Raman laser in a methane-filled negative-curvature fiber[J]. Optics Express, 2018, 26(5): 5609-5615.
[20] Astapovich M S, Gladyshev A V, Khudyakov M M, et al. Watt-level nanosecond 4.42-μm Raman laser based on silica fiber [J]. IEEE Photonics Technology Letters, 2019, 31(1): 78-81.
[21] Huang W, Li Z X, Cui Y L, et al. Efficient, watt-level, tunable 1.7 μm fiber Raman laser in H_2-filled hollow-core fibers[J]. Optics Letters, 2020, 45(2): 475-478.
[22] Wang Y Z, Dasa M K, Adamu A I, et al. High pulse energy and quantum efficiency mid-infrared gas Raman fiber laser targeting CO_2 absorption at 4.2 μm[J]. Optics Letters, 2020, 45(7): 1938-1941.
[23] Zhu X Y, Wu D K, Wang Y Z, et al. Delivery of CW laser power up to 300 watts at 1080 nm by an uncooled low-loss anti-resonant hollow-core fiber[J]. Optics Express, 2021, 29(2): 1492-1501.
[24] Wang Y Z, Schiess O T S, Amezcua-Correa R, et al. CO_2-based hollow-core fiber Raman laser with high-pulse energy at 1.95 μm[J]. Optics Letters, 2021, 46(20): 5133-5136.
[25] Zhang X, Peng Z G, Dong Z H, et al. High-power mid-infrared 2.8-μm ultrafast Raman laser based on methane-filled anti-resonant fiber[J]. IEEE Photonics Technology Letters, 2022, 34(19): 1007-1010.
[26] 黄威, 李智贤, 崔宇龙, 等. 反共振空芯光纤中氘气受激拉曼散射实验研究[J]. 中国激光, 2020, 47(1): 0101001.
Huang W, Li Z X, Cui Y L, et al. Experimental research on stimulated Raman scattering of deuterium gas in anti-resonance hollow-core fibers[J]. Chinese Journal of Lasers, 2020, 47(1): 0101001.
[27] 李昊, 黄威, 裴闻喜, 等. 连续波 1.7 μm 全光纤气体拉曼激光光源[J]. 光学学报, 2021, 41(3): 0314001.
Li H, Huang W, Pei W X, et al. Continuous-wave 1.7 μm all-fiber gas Raman laser source[J]. Acta Optica Sinica, 2021, 41(3): 0314001.
[28] 孙青. 基于空芯光子晶体光纤的气体受激拉曼散射效应[D]. 合肥: 中国科学技术大学, 2009.
Sun Q. Stimulated Raman scattering based on gas-filled hollow-core photonic crystal fiber[D]. Hefei: University of Science and Technology of China, 2009.
[29] Hanson F, Poirier P. Stimulated rotational Raman conversion in H_2, D_2, and HD[J]. IEEE Journal of Quantum Electronics, 1993, 29(8): 2342-2345.

2.15 μm All-Fiber Gas Raman Laser Source

Li Ziyan[1], Pei Wenxi[1,2], Li Hao[1,2], Huang Wei[1,2], Li Xuanxi[1,2], Wang Zefeng[1,2,3*], Chen Jinbao[1,2,3]

[1]*College of Advanced Interdisciplinary Studies, National University of Defense Technology, Changsha* 410073, *Hunan, China*;
[2]*Nanhu Laser Laboratory, National University of Defense Technology, Changsha* 410073, *Hunan, China*;
[3]*State Key Laboratory of Pulsed Power Laser Technology, Changsha* 410073, *Hunan, China*

Abstract

Objective Laser at 2.15 μm band has important applications in many fields. For example, it is located in the transmission window of the atmosphere and has remarkable transmittance in smoke, which makes it more reliable for data transmission in some special contexts. It has also realized the measurement of factors in the atmospheric environment, such as wind velocity, carbon dioxide, and water vapor. Lasers around 2.15 μm band are ideal pump sources for generating mid-infrared laser through nonlinear frequency conversion. Fiber lasers have great advantages in beam quality,

stability, and portability. At present, most fiber laser at 2 μm band is generated by holmium-doped or thulium-doped fiber lasers. However, on one hand, due to the enormous decreases in the absorption and emission cross sections of Ho^{3+} and Tm^{3+} beyond 2.1 μm, the wavelength is difficult to expand to over 2.1 μm, and the power scaling is also restricted by insufficient gain. On the other hand, various nonlinear effects, such as self-phase modulation and stimulated Raman scattering (SRS), will lead to spectral broadening under high pump power, which restricts the applications of the lasers. Gas SRS in hollow-core fibers (HCFs) has been proved to be an effective method for expanding laser wavelengths. HCFs can provide an ideal environment for the interaction between the gas and the pump laser. Gas SRS in HCFs combines the advantages of traditional fiber lasers and gas lasers, such as high beam quality, high damage thresholds, narrow linewidths, and convenient heat management. In this paper, we report an all-fiber gas Raman laser at 2.15 μm band through fusion splicing between a solid-core fiber and an HCF. This paper provides a novel method to generate fiber lasers beyond 2.1 μm.

Methods The 2.15 μm fiber gas Raman laser is realized based on the pure rotational SRS of deuterium filled in a 25.8 m long HCF. The 1971 nm pump laser is directly coupled into the HCF through the splicing between the solid-core fiber and the HCF. The output end of the HCF is sealed in a gas cell when it is filled with deuterium. After the internal gas pressure becomes balanced, the HCF is quickly withdrawn and spliced to the solid-core fiber, which forms an all-fiber gas cell. The Raman laser caused by the Fresnel reflection of the splice is well prevented from inducing damage to the pump source by introducing a self-written long-period fiber grating (LPG) in the solid-core fiber.

Results and Discussions The self-written LPG functions well as an isolator of the Raman laser caused by Fresnel reflection, and the depth at 2147.1 nm is around −8 dBm [Fig. 1(c)]. This means most part of Fresnel reflection is attenuated, and thus the pump source can be protected from being damaged by the Raman laser. The splice loss at the input end and the output end is ∼1.42 dB and ∼1.00 dB, respectively. The gas pressure in the all-fiber gas cell is calculated to be around 1.4 GPa. Two first-order Raman lines are obtained in the experiment (Fig. 3). The 2147.1 nm Raman line is first generated because its threshold is lower than that of the 2043.6 nm Raman line. As the coupled pump power increases, part of the pump power is converted to 2043.6 nm Raman laser. With the increase in the pump repetition frequency, the pump laser has lower peak power (inversely proportional to the repetition frequency). Therefore, higher average pump power is necessary to exceed the Raman threshold, and more pump power is needed to generate Raman laser with the repetition frequency increasing [Fig. 4(a)]. Although the peak power is lower at the repetition frequency of 1.5 MHz and 2.0 MHz, the available pump power is much higher than that at 0.5 MHz and 1.0 MHz. Thus, the Raman power at these two repetition frequencies (1.5 MHz and 2.0 MHz) is much higher than that at the other two repetition frequencies. The power characteristics under different pumping pulse widths are also studied in detail (Fig. 5). Finally, a maximum Raman power of ∼0.87 W at 2.15 μm is obtained [Fig. 4(a)] with a corresponding optical-to-optical conversion efficiency of 19% restricted by a high Raman threshold. The Raman power and conversion efficiency can be enhanced by optimizing the splice loss and fiber length of the HCF.

Conclusions In this paper, we report a 2.15 μm all-fiber gas Raman laser. The all-fiber gas cell is obtained through the fusion between a single-mode solid-core fiber and a hollow-core photonic crystal fiber, and the Raman laser caused by the Fresnel reflection of the splice is well prevented from inducing damage to the pump source by introducing a self-written LPG in the solid-core fiber. Pumped by a 1971 nm pulse fiber amplifier, a maximum Raman power of ∼0.87 W at 2147.1 nm is obtained with a corresponding optical-to-optical conversion efficiency of 19% restricted by a high Raman threshold. This paper provides a novel method to realize a fiber laser source beyond 2.1 μm.

Key words lasers; fiber gas Raman lasers; hollow-core fibers; stimulated Raman scattering